

Investigation of Crystal Size Distribution in Purification of Terephthalic Acid from Polyester Textile Industry Waste by Reactive Crystallization

Bekti Marlana^{1,2*}, Hary Sulisty¹, and Rochmadi Rochmadi¹

¹Department of Chemical Engineering, Universitas Gadjah Mada, Jl. Grafika 2, Yogyakarta 55284, Indonesia

²Center for Standardization and Industrial Pollution Prevention Services, Jl. Kimangunsarkoro No. 6, Semarang 5013, Indonesia

* **Corresponding author:**

email: bektimarlena@mail.ugm.ac.id

Received: December 31, 2022

Accepted: March 29, 2023

DOI: 10.22146/ijc.80820

Abstract: The purification of terephthalic acid recovered from an alkali-reduction wastewater by reactive crystallization was investigated. The crude terephthalic acid was reacted with sodium hydroxide solution to form a salt of disodium terephthalate, then acidified with sulfuric acid to get the terephthalic acid with higher purity. The effects of time, pH, concentration, and flow rate of secondary feed solutions, temperature, and stirring rate on crystal size distribution (CSD) of terephthalic acid precipitate were investigated. The results showed that CSD was influenced by the concentration of reactants and the pH solution. On the other hand, time, temperature, flow rate of secondary solution, and stirring rate had no significant effects on the CSD, which the mean size of crystals $\pm 3 \mu\text{m}$. The mean size of crystals at solution pH 5, 4, and 3 were 6.03, 9.42, and 10.34 μm , respectively; meanwhile, at concentrations of 0.5, 0.3, and 0.1 M, were 7.57, 3.24, and 3.09 μm , respectively. The semi-batch reactive crystallization with double-feeding at constant pH and temperature resulted in monodispersed crystals. However, this method must be carried out more than once for terephthalic acid purification, intended for polyethylene terephthalate (PET) polymerization.

Keywords: crystal size distribution; purification; reactive crystallization; terephthalic acid

■ INTRODUCTION

Polyester is the most widely used synthetic fiber due to its low production cost and good fiber properties. Still, it has poor wear comfort because of its low moisture absorption and stain removal ability. Therefore, some approaches have been developed to improve the hydrophilicity of polyester fiber [1]. The strong alkaline treatment of polyester leads to the rupture of ester bonds. It increases the number of polar functional groups of alcohol and carboxylic acid on the fiber surface [2].

On the other hand, alkali treatment causes hydrolysis of the ester bond. The chain hydrolysis of polyethylene terephthalate (PET) with sodium hydroxide produces disodium terephthalate, which is highly soluble in water. This alkali process also causes changes in fabric weight, strength, wettability, and aesthetics [3]. The large amount of weight loss in this hydrolysis process is known as the weight reduction process.

The wastewater from this process has extreme characteristics such as a very alkaline pH (> 12.8) and a high organic concentration (COD of 20,000–100,000 mg/L) [4]. Therefore, some researchers have studied the recovery of terephthalic acid as one of the attractive treatments for this wastewater [5]. Terephthalic acid recovery is carried out by acidifying wastewater to precipitate the terephthalic acid. This method is known as precipitation or reactive crystallization. In this process, the formation of a crystal or solid product is initiated with high supersaturation conditions which are obtained from the chemical reaction between the soluble reactants [6]. Supersaturation is a driving force for nucleation which is the initial formation of a solid phase or crystal. The growth of the crystal increases the crystal size.

Industrially, crystalline product quality and properties are determined by the crystal size distribution (CSD), morphology, and purity [7-8]. Chemical

composition, as represented by the chemical purity and impurity levels, can change the crystal properties, such as the mechanical, electrical, thermal, and optical properties. Control of impurities is also essential in many industries, especially in the food and pharmaceutical industries, where product purity should reach the strict specifications required for human use [9]. The crystal size distribution (CSD) and crystal habit or morphology can change product and bulk properties such as dusting, dissolution rate, compressibility, and flowability [10]. They also influence the efficiency of downstream processes such as filtration, centrifugation, and drying [11].

The crystallization process control is important to acquire products with desired and reproducible properties. Poor product properties can cause extra processing steps, which will increase manufacturing costs and be time-consuming [12]. Obtaining the desired particle size can often be challenging due to the interaction among various process parameters. A series of techniques, including mathematical modeling tools, have been applied to predict and control particle size and distribution [13].

The CSD on crystallization can be predicted using the Population Balance Equation (PBE). PBE is an equation that represents the balance of the number of particles in a specific state. For a batch crystallizer or a semi-batch crystallizer with assumptions that the system is perfectly mixed and there is no net inflow or outflow of crystals. The PBE can be written in Eq. (1).

$$\frac{\partial n}{\partial t} = G \frac{\partial n}{\partial L} \quad (1)$$

Eq. (1) requires an initial condition and a boundary condition. The initial condition of $n(L, 0)$ for unseeded batch suspension crystallizer uses the size distribution of crystal at the time of the first appearance crystals. The boundary condition $n(0, t)$ is the nuclei population density (n_0) and is related to the nucleation rate (B), as shown in Eq. (2).

$$n(0, t) = n_0(t) = \frac{B(t)}{G(0, t)} \quad (2)$$

Nucleation kinetics and crystal growth rate cannot be predicted theoretically, and in practice, they must be measured and correlated empirically with environmental

conditions, such as concentration and temperature, using a power law model, as shown in Eq. (3) and (4).

$$B = k_N \Delta c^b \quad (3)$$

$$G = k_G \Delta c^g \quad (4)$$

where B is nucleation rate, k_N is nucleation rate constant, Δc is supersaturation, exponent b is an order of nucleation, G is crystal growth, k_G is growth rate constant, and exponent g is an order of growth. The value of the primary nucleation kinetic constant b varies in the range of 1–10 [14]. Meanwhile, the value of growth kinetic constant g , in general, is $1 \leq g \leq 2$, and $g > 2$ only for sparingly soluble compounds [6]. Studies of CSD on semi-batch reactive crystallization were conducted by single feed [15-17] or double feeds [18], as well as double feeds at constant pH by adding external acid or basic [19-20].

Studies on the purification and recovery of terephthalic acid from alkali weight reduction wastewater using reactive crystallization [5] and cooling crystallization [21] focused on terephthalic acid's purity. However, research on CSD of terephthalic acid using reactive crystallization, especially from recovery weight reduction wastewater, is still scarce.

It is assumed that at a constant pH, disodium terephthalate will react with sulfuric acid to form terephthalic acid, which increases the concentration of terephthalic acid in the solution. It is expected to increase the crystal growth rate and size. Thus, the work presented in this paper aimed to study the effect of the crystallization processes (time, pH, temperature, concentration, flow rate of secondary solutions, and stirring speed) on the crystal size distribution. The crystallization process was conducted in conditions of semi-batch, constant solution pH, and constant solution temperature (isothermal) by adjusting the feeding of the secondary solution of reactants.

■ EXPERIMENTAL SECTION

Materials

The weight-reduced wastewater was collected from a textile industry in Central Java Province, Indonesia. The weight-reduced wastewater was added with activated carbon and then acidified to pH 2 [5]. The

terephthalic acid precipitate was then filtered and dried to produce crude terephthalic acid, having the characteristics shown in Table 1.

Analytical grade chemicals used in reactive crystallization were sulfuric acid (Merck, 95–97%), charcoal activated (Merck), and sodium hydroxide (Merck, 99%).

Instrumentation

The semi-batch crystallization system with double-feeding reactants for the study of reactive crystallization of terephthalic acid is illustrated in Fig. 1. Experimental setup consisted of a reactor, a mechanical stirrer, two peristaltic pumps, and a pH meter. A glass beaker of 1 L

equipped with four baffles (0.1 of beaker diameter) and four blades of paddle impeller stirrer (0.3 of beaker diameter) was used as a reactor. The stirrer was driven by IKA RW 20 digital overhead stirrer. HI9890 pH meter was connected to a computer to monitor and save the data of pH and temperature during the process. A Cole Palmer water bath was used to maintain and control the process temperature. Masterflex C/L peristaltic pumps were employed to feed the secondary disodium terephthalate and sulfuric acid solutions to the reactor. The crystal size distribution was determined using a Particle Size Analyzer (PSA) Horiba Partica LA 960 V2.

Table 1. Characteristics of crude terephthalic acid

No	Parameter	Crude terephthalic acid	Unit	Method
1	Acid number	572.500 ± 7.500	mg KOH/g	Titration
2	Ash	229.900 ± 5.200	ppm (w/w)	Gravimetry
3	Moisture	6.160 ± 0.220	% (w/w)	Gravimetry
4	Alkali transparency T-400	73.350	%	Spectrophotometry
5	Mean size	21.335 ± 0.065	µm	Laser diffraction
6	Metal contents			
	Mn	2.890 ± 0.119	ppm (w/w)	Atomic absorption
	Ni	0.279 ± 0.219	ppm (w/w)	spectroscopy (AAS)
	Co	0.020 ± 0.001	ppm (w/w)	
	Cr	1.219 ± 0.462	ppm (w/w)	
7	Iron (Fe)	17.556 ± 4.239	ppm (w/w)	AAS
8	Color in 5% dimethylformamide	51.650	-	spectrophotometry

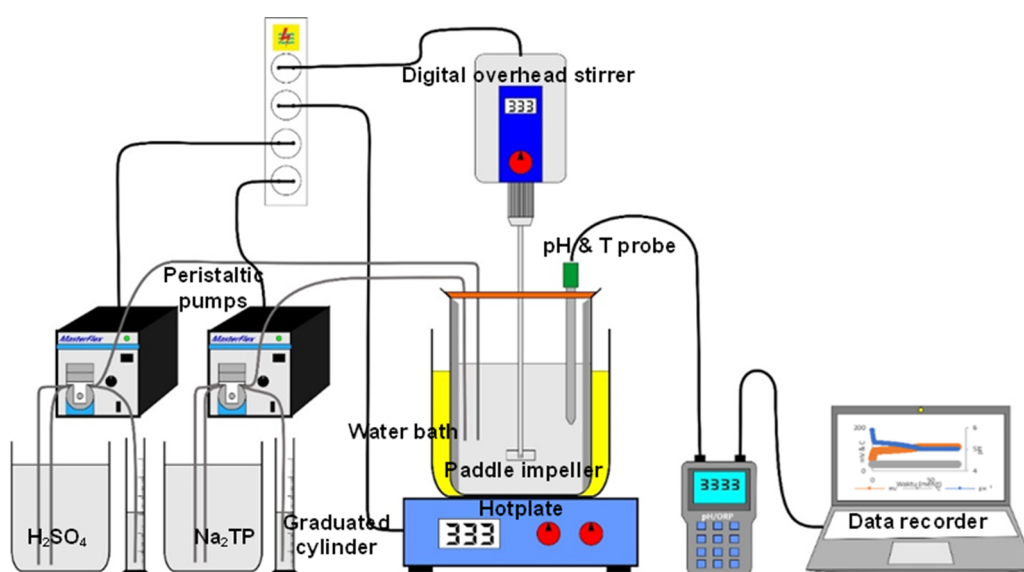


Fig 1. Experimental setup

Procedure

The amount of 400 mL of 0.06 M primary disodium terephthalate solution was put into a glass beaker with a volume of 1 L as a reactor. It was acidified with 0.5 M sulfuric acid solutions (approximately 50 mL) until the targeted pH was reached. At this point, initial time sampling was carried out by taking 25 mL of solution.

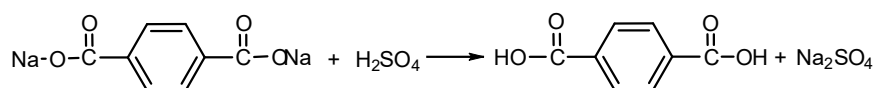
Secondary solutions of 0.5 M disodium terephthalate and 0.5 M sulfuric acid solutions were added continuously to the reactor (primary solution) using two peristaltic pumps in an equal amount between terephthalate and sulfuric acid. The addition of this second solution did not affect the pH of the solution due to an equimolar amount of terephthalate and sulfuric acid. The initial volume of the primary solution at the targeted pH was approximately 450 mL. The volume of sulfuric acid added at a feeding rate of 1 mL/min was 30 mL, and the volume of disodium terephthalate added was also 30 mL. The final total volume was 385 mL after subtracting the entire sample volume taken (125 mL). Samples were taken at 5, 10, 20, and 30 min after secondary solutions were charged into the primary solution. The pH and temperature of the reaction were monitored and manually controlled by manipulating the flow rate of the H₂SO₄ solution.

Each sample was filtered, and the precipitated terephthalic acid was oven-dried at 70 °C and then weighed (until constant). The dried sample was analyzed using a PSA, which shows the characteristic dimension of the crystals in the volume equivalent size.

RESULTS AND DISCUSSION

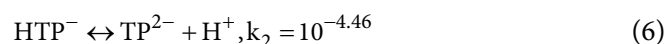
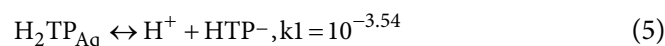
The Chemical Reaction of Disodium Terephthalate with Sulfuric Acid

The reaction of disodium terephthalate with sulfuric acid is shown in Scheme 1. Disodium terephthalate and sulfuric acid are ionic reactants in an aqueous solution, which essentially reacts very fast, producing a terephthalic acid precipitate [22]. The reactive crystallization mechanism consists of several steps. The first step is



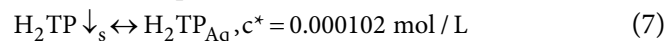
Scheme 1. The reaction of disodium terephthalate with sulfuric acid

terephthalic acid formation by reacting disodium terephthalate with sulfuric acid. The solution dissolves the terephthalic acid into ionic terephthalates (Eq. 5-6) [23].



where H₂TP, HTP⁻ and TP²⁻ indicate the neutral, dissociated, and twice dissociated forms of terephthalic acid, respectively. The neutral form is called free acid. The relative amounts of the three ions depend on the pH solution. The concentration of each species at equilibrium can be calculated by the fraction or alpha (α) by comparing its concentration with the total concentration of phthalate ions with the help of the dissociation constant [24].

Fig. 2 shows the speciation of terephthalic acid as a function of the pH solution. The two intersection points of these curves were pK₁ and pK₂. The free acid of terephthalic acid forms a precipitate when its concentration exceeds the solubility value at equilibrium conditions (Eq. 7).



The mass balance of total terephthalates in the solution was calculated from concentrations of terephthalate ions (HTP⁻ and TP²⁻) and free acid H₂TP using Eq. (8).

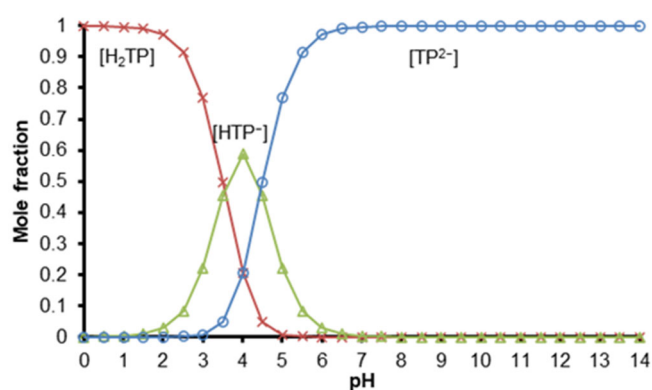


Fig 2. Mole fractions of ionic species of terephthalate as a function of solution pH

$$[\text{TP}_{\text{TOTAL}}] = [\text{TP}^{2-}] + [\text{HTP}^-] + [\text{H}_2\text{TP}] \quad (8)$$

The electroneutrality balance of all species in the solution was calculated using Eq. (9).

$$[\text{H}^+] = 2[\text{TP}^{2-}] + [\text{HTP}^-] + [\text{HSO}_4^-] + 2[\text{SO}_4^{2-}] + [\text{OH}^-] \quad (9)$$

Eqs. (5-9), together with measured pH data and total sodium concentration, were used to calculate the concentrations of terephthalate ions (TP^{2-} and HTP^-), free terephthalic acid (H_2TP) in the solution, and solid, with the assumption that the solution was an ideal solution at equilibrium and sulfuric acid was a strong acid.

The pH profiles, concentrations of terephthalic acid in solution, and terephthalic acid solid at the addition of sulfuric acid into 100 mL disodium terephthalate solution with the same concentration (0.45 M) are shown in Fig. 3.

Adding sulfuric acid decreased the solution pH and the concentration of disodium terephthalate. The gentle slope of the pH curve (red line) indicated the occurrence of spontaneous nucleation. Then, it was followed by the steep slope in which the solution was sensitive to pH (around $\text{pH} = 4$), where disodium terephthalate was equimolar to sulfuric acid. At this stage, adding a small amount of sulfuric acid (± 3 mL) drastically changed the pH from 4.64 to 2.85.

The terephthalic acid is sparingly soluble in water with a solubility of 0.000102 M. If the concentration of terephthalic acid exceeds the solubility value at equilibrium conditions, then the solid terephthalic acid forms. The solubility of terephthalic acid or concentration of terephthalic acid in the solution (H_2TP) curve (green line) was assumed constant regardless of the pH of the solution.

The supersaturation condition of terephthalic acid was the driving force of crystallization which consisted mainly of nucleation and crystal growth. The relationship between nucleation and growth and agglomeration or breakage of crystals certainly affected the final product of CSD [8].

CSD of Crude Terephthalic Acid

The CSD of crude terephthalic acid used in this experiment is shown in Fig. 4. The graph shows that CSD stretched from 0.5–700 μm , with two peaks located at 5.5 μm by 4.1% and 29.9 μm by 3.9%. It indicated that the

crude terephthalic acid had a very broad crystal size with a mean size of 26.83 μm .

CSD of Terephthalic Acid from Double Feed Semi-batch Reactive Crystallization at Constant pH and Temperature

The primary disodium terephthalate solution was acidified with sulfuric acid solutions until the targeted pH was reached. At this point, initial time sampling was carried out. Secondary disodium terephthalate and sulfuric acid solution were added equimolar by keeping the pH solution constant.

Adding an equimolar secondary solution of disodium terephthalate and sulfuric acid at constant pH was expected to increase the concentration of terephthalic acid in the reactor for crystal growth. The feeding time of secondary solutions at constant pH was conducted for 30 min.

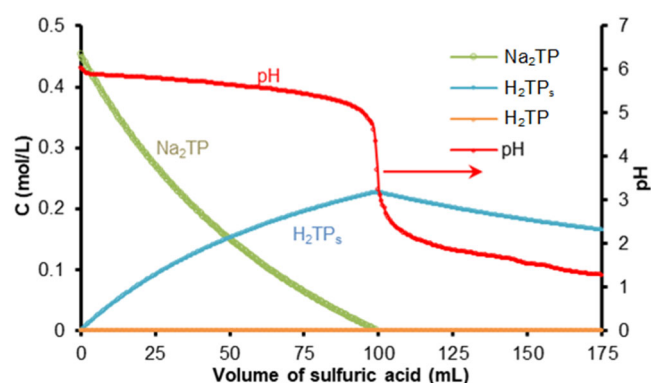


Fig 3. Equilibrium concentrations and pH of 0.45 M disodium terephthalate 100 mL with 0.45 M sulfuric acid additions

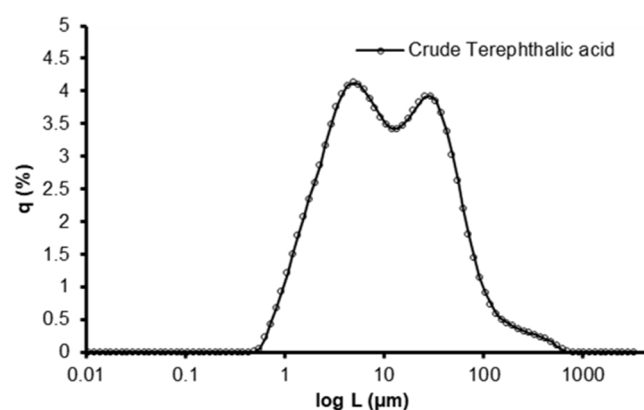


Fig 4. CSD of crude terephthalic acid

Effect of feeding time

The experiments were conducted at a solution pH of 5, at a concentration of a secondary solution of 0.5 M, and at a temperature of 30 °C at various feeding times.

The addition of secondary solutions (in equimolar reactants) increased the amount and number of crystals. Still, the size distribution was similar at various feeding times, from 0 to 30 min, as shown in Fig. 5. This means that feeding time did not influence the size of crystals. It was apparent that the crystallization process (nucleation and crystal growth) occurred very fast in the time scale of seconds; meanwhile, samples taken from the solution were within 5–10 min intervals. The short time scale of the crystallization process was probably due to the high supersaturation of terephthalic acid due to the low solubility of the terephthalic acid in water [25]. The high supersaturation caused the spontaneous primary nucleation to be more dominant than the growth of crystals.

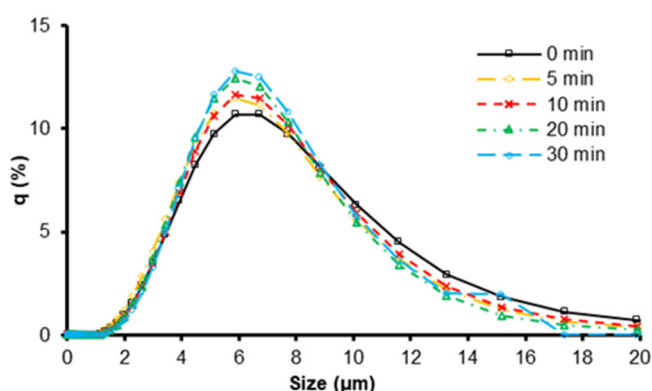


Fig 5. CSD of terephthalic acid at conditions of pH 5 and T 30 °C

Effect of solution pH

The solution pH was varied to 3, 4, and 5, as shown in Fig. 7. During the experiment, the feed rate was controlled manually at a fixed pH. Controlling the secondary solution feed rate was relatively easy at solution pH 5, compared to solution pH 4 and 3, which were sensitive to small fluctuations in the acid feed rate. It is illustrated in Fig. 6.

The fluctuations in the concentration of H⁺ ions at pH 3, 4, and 5 were between 3.05–2.96, which equaled CH⁺ = 9.10⁻⁵ (g ion/L); between 4.12–3.88, which equaled CH⁺ = 2.4.10⁻⁵ (g ion/L), and between 5.02–4.99, which equaled CH⁺ = 3.10⁻⁷ (g ion/L).

As mentioned above, the terephthalic acid was dissociated in water, and the species of ion terephthalates was a function of the solution pH. Fig. 2 shows that the free acid from terephthalic acid began to increase at pH 5.5, increasing with the decrease in the solution pH. Therefore, decreasing the pH can increase

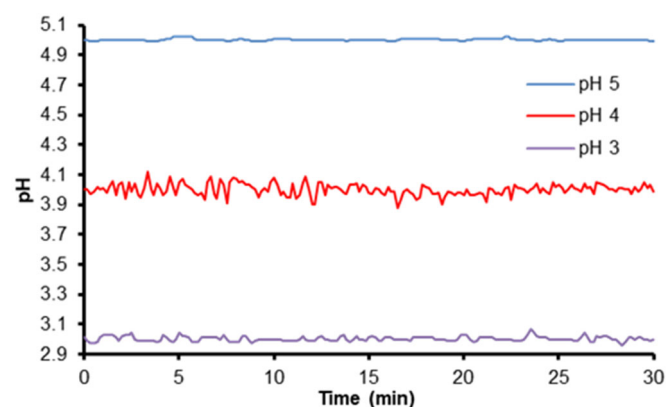


Fig 6. pH fluctuations during experiments

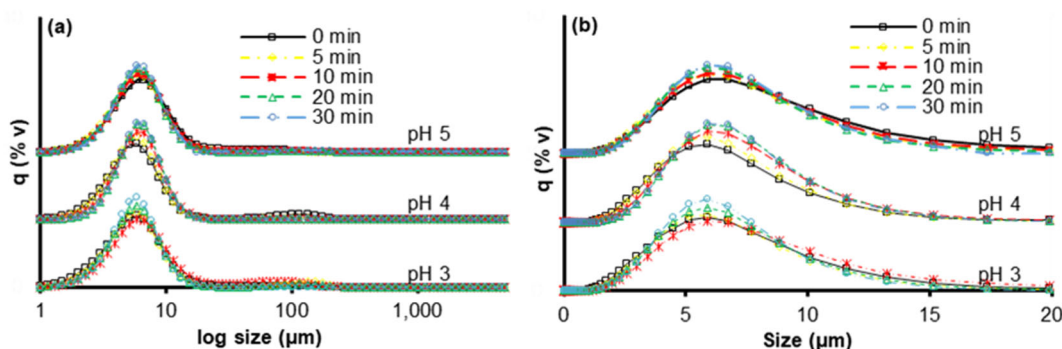


Fig 7. CSD of terephthalic acid at pH variations

the concentration of terephthalic acid as well as supersaturation. When the supersaturation was high, and the solubility was low, the crystallization process was dominated by nucleation, which produced fine crystals. On the other hand, a decrease in the pH of the solution can increase the accumulation of fine crystals [26-27]. Aggregation occurred because there were terephthalate ions (TP^{2-} and HTP^-) and undissociated terephthalate (H_2TP) when lattice crystals were formed so that the surface of the crystal was easily charged.

The logarithmic scale has a broader span of crystal size, as shown in Fig. 7(a). Because of this wide span, CSD in the logarithmic scale showed the presence of two peaks (bimodal) at pH solution of 4 and 3 in the early minutes of the experiments. The primary peak dominated the crystal distribution in a smaller size ($\pm 10 \mu m$), while the second peak appeared in a larger size ($\pm 130 \mu m$), but its frequency was relatively small. Meanwhile, the normal scale (Fig. 7(b)) showed a tendency to increase the number of crystals, indicated by an increase in the peak distribution concerning time.

Large-sized crystals at acidic pH probably came from the aggregation of terephthalic acid. Adding a secondary solution at a constant pH can reduce the accumulation towards a more uniform crystal distribution. It was indicated by the disappearance of the secondary peak (which is essentially small), leading to an increase in the height of the primary peak. Similar studies with double feeds at constant pH showed that changes in CSD indicated the occurrence of aggregation [20].

Fig. 8 shows that the mean crystal size of the terephthalic was increased as the pH solution decreased from 5 to 3. In this case, the pH solution = 5 was chosen for further experiments because it was more stable and easier to control the pH solution. A decrease in pH means that the rise of H^+ concentration (more acidic solution) essentially affected the saturated concentration of terephthalic acid and consequently influenced the size of the terephthalic crystal. Eqs. (3) and (4) can be used to describe this phenomenon.

The reactive crystallization by changing the solution pH (pH swing) was widely applied to produce a less soluble acid or base from a salt [8], usually applied for a

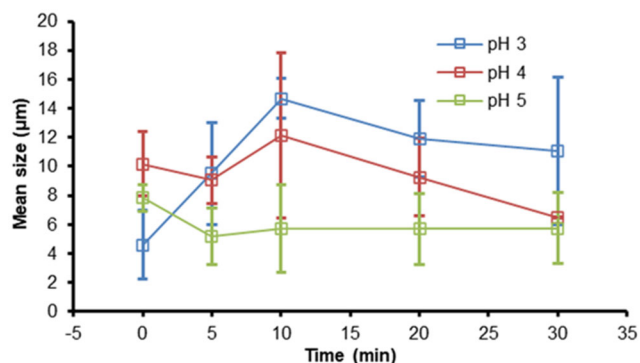


Fig 8. The mean size of terephthalic acid at variations of pH

single-feed semi-batch reactive crystallization [26]. In general, the acid solution produced fine crystals because of rapid nucleation and increased agglomeration. Meanwhile, the double-feed semi-batch crystallization at constant pH showed that pH variation contributed to aggregation [20] and morphology [19].

Effect of secondary solutions concentration

Higher secondary solution concentrations increased the crystal size of terephthalic acid, as presented in Fig. 9. A lower concentration of secondary solution produced a narrower distribution of terephthalic crystals; meanwhile, a higher concentration made a broadened distribution. The secondary solution concentrations affected mean crystal sizes. The concentrations of 0.5, 0.3, and 0.1 M resulted in a mean size of 7.13–8.75, 2.93–4.20, and 3.02–3.20 μm , respectively. A lower concentration led to a lower mean crystal size and variance coefficient, indicating a more uniform size.

A higher concentration of reactants (in secondary solutions) produced a higher terephthalic acid supersaturation condition, which was a driving force for nucleation followed by consecutive and rapid growth. After nucleation, followed by the growth of the crystal, the concentration of the solution decreased gradually, leading to saturated concentration, in which the growth rate stopped.

Similar results were obtained by Tai and Chen [20], reporting that under high supersaturation conditions, the crystal size increased due to the high growth rate. The experiment was conducted for the precipitation of

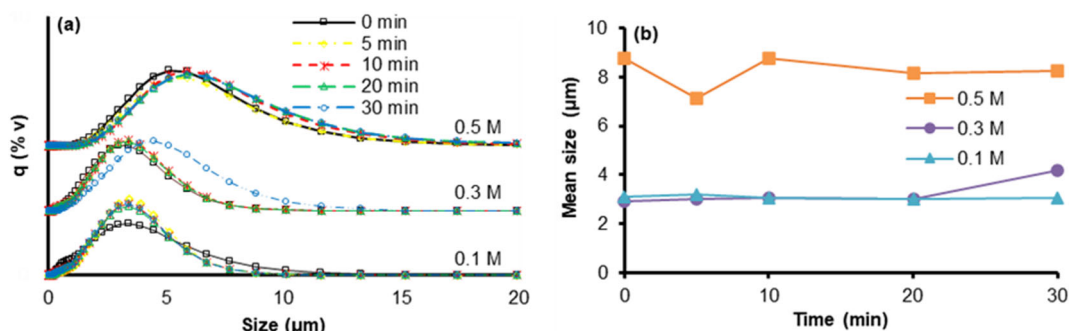


Fig 9. (a) Distribution and (b) size of crystals of terephthalic acid at the variation of secondary solution concentrations

calcium sulfite hemihydrate by using double feeds and operating at a constant pH. These conditions resulted in nucleation rates that were not too high, and supersaturation conditions controlled the crystal growth rate.

Different results were shown by Rewatkar et al. [15] regarding the precipitation of calcium oxalate and Caro et al. [16] regarding the precipitation of salicylic acid. These previous studies showed that the higher the reactant concentration was used, the finer the crystal size was obtained. However, these studies were carried out on single-feed reactive crystallization systems. Furthermore, a study on reactive crystallization conducted by Utomo et al. [28] comparing single feed and double feeds showed that the single feed system produced a smaller and wider crystal size distribution than the double feed systems.

Effect of feeding rate

The feeding rate affects the supersaturation. An increase in the feeding rate increases local supersaturation, increasing the nucleation rate.

The results showed that a feeding rate of 1 to 3 mL/min did not significantly affect the CSD of

terephthalic acid. It is shown in Fig. 10(a), where the CSDs overlapped. The feeding rate of 1, 2, and 3 mL/min resulted in a mean size of 2.92–3.76, 3.01–3.87, and 3.12–4.07 μm, respectively.

The same result was observed by Han and Louhi-Kultanen [17] and Tai and Chen [20], stating that increasing feed speed can increase supersaturation and nucleation. Still, if the supersaturation was high, then the effect of feed speed was small enough, so it was not significant to be analyzed further. To some extent, nucleation was challenging to be controlled by controlling the feeding rate, especially in unseeded operations [29].

Effect of temperature

The experiments were conducted under isothermal conditions at three temperature variations of 30, 50, and 70 °C.

The tendency of crystal distributions varies with time; at 30 °C, the peak tended to shift to the right; at 50 °C, it tended to increase, while at 70 °C, it had a very close value. Temperature affected the nucleation rate. The nucleation rate increased with increasing the temperature and the degree of supersaturation. In addition, the

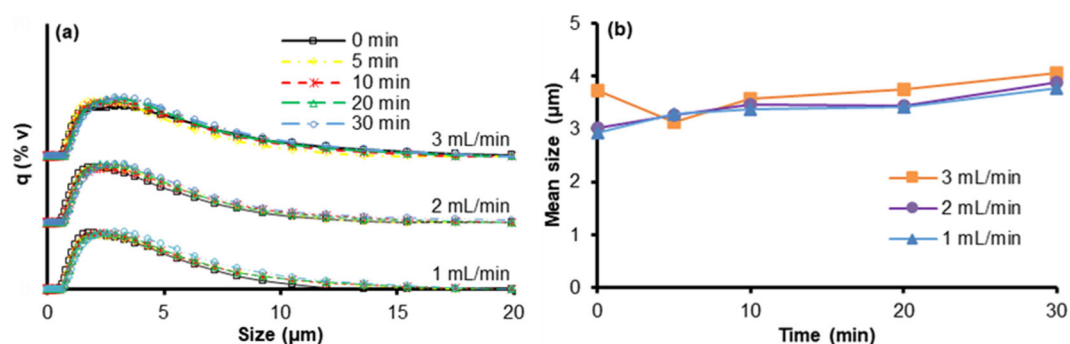


Fig 10. (a) Distribution and (b) mean size of crystals of terephthalic acid at the variation of feeding rates

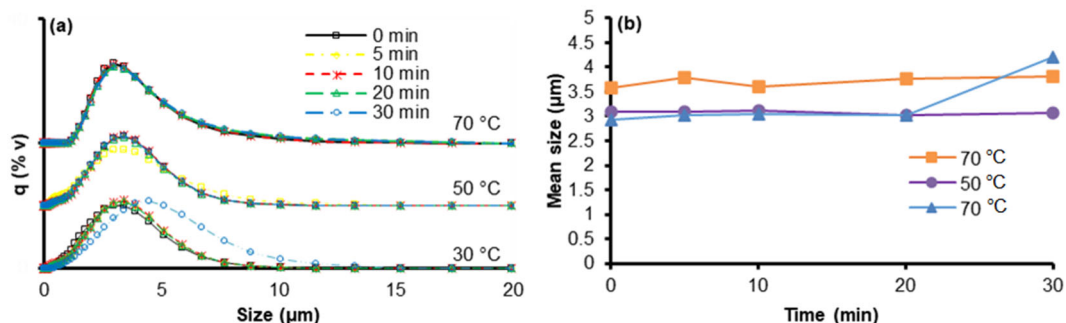


Fig 11. (a) Distribution and (b) mean size of crystals of terephthalic acid at variations of temperatures

solubility of terephthalic acid increased with increasing the solution temperature. The solubility of terephthalic acid in water from experiments at various temperatures compared to a previous study by Park and Sheehan [30] is presented in Fig. 12.

A higher temperature caused a higher terephthalic acid (saturated) solubility, consequently lowering the supersaturation conditions ($\Delta c = \text{initial concentration} - \text{saturated concentration}$). Finally, it decreased the nucleation and increased the crystal growth, producing a larger crystal size. However, Fig. 11(b) indicates that terephthalic acid precipitation temperature only significantly affected the crystal size. The competition between the increasing reaction rate and the solubility with the solution temperature was specific for each system [22]. The competition seems negligible for the reactive crystallization of terephthalic acid; therefore, the temperature significantly affected CSD.

Effect of the stirring rate

Theoretically, crystal growth is influenced by mass transfer rate, as confirmed by Eq. (4). One factor that affects the mass transfer rate is the stirring rate, besides

the solution properties.

This study conducted experiments at 120, 300, and 420 rpm stirring rates. Fig. 13(b) shows that the mean crystal size slightly decreased with the increase of stirring rate from 120 to 420 rpm, although it was not very significant. This result agreed with the research on the precipitation of hydroxyapatite by Tourbin et al. [31], which showed that crystal size increased at a stirring rate of 120–600 rpm. However, the results of Caro et al. [16] showed that crystal size increased at a stirring rate of 100–400 rpm and decreased at a stirring

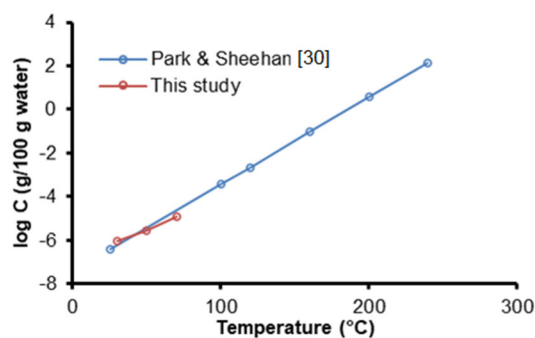


Fig 12. Terephthalic acid solubility at various temperatures

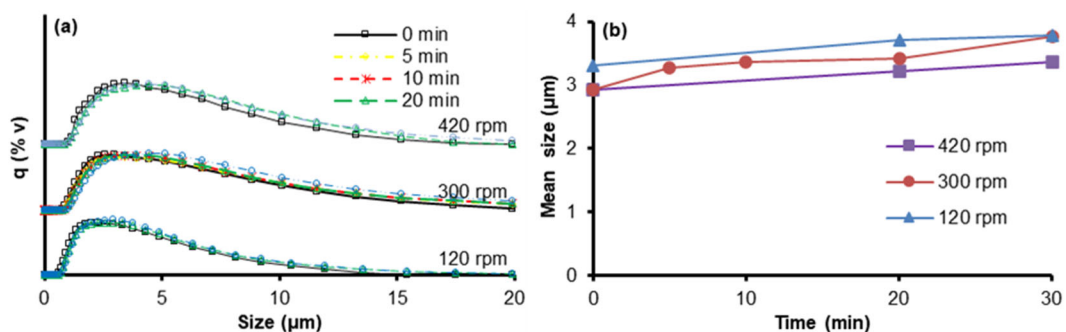


Fig 13. (a) Distribution and (b) mean size of crystals of terephthalic acid at the variation of stirrer stirring rates

Table 2. Characteristics of terephthalic acid by reactive crystallization

No	Parameter	Terephthalic acid	Standard	Unit	Method
1	Acid value	675.338	675 ± 2	mg KOH/g	Titrimetry
2	Ash content	31.047	max 15	ppm (w/w)	Gravimetry
3	Water content	0.028	max 0.15	% (w/w)	Gravimetry
4	Metals	1.115	10	ppm	
5	Fe	0.472	2	ppm	Atomic absorption
6	Co, Mo, Ni, Ti, Mg	0.643	max 1	ppm	spectroscopy
7	4-CarboxyBenzaldehyde (4-CBA)	73.141	max 25	ppm	Chromatography
8	<i>p</i> -Toluic acid	112.379	max 150	ppm	Chromatography
9	Color in 5% dimethylformamide	8.580	max 10	APHA	Spectro

speed of 800–1600 rpm.

Essentially, the rise of the stirring rate enhances the degree of turbulence, which increases the mass transfer rate and finally increases the crystal growth rate. However, the results showed that the stirring rate only slightly affected the crystal size distribution, where the mean crystal size remained as the stirring rate increased. It means that the crystal growth step did not control the overall crystallization process.

The semi-batch reactive crystallization with double-feeding reactants at constant pH and temperature forms nearly the same size crystals. It shows that this method can be used to obtain monodispersed crystals.

Purity of Terephthalic Acid

Terephthalic acid obtained from this experiment was characterized and compared to the standard of commercial terephthalic acid [32] to demonstrate its potential industrial application.

According to ASTM D7976 Standard for purified terephthalic acid, the terephthalic acid purity requirement for PET polymerization is a 4-CBA content of 25 ppm max [21]. The presence of 4-CBA impurities reduces the rate of polymerization in polyester production because the aldehyde functional group in 4-carboxy benzaldehyde cannot react with ethylene glycol in the polymerization process, which limits the polyester chain so that the molecular weight becomes low [33-34].

The results show that reactive purification still contains 4-CBA, which is still relatively high at 73 ppm, and ash content of 31.05 ppm (Table 2). Therefore, the purification of terephthalic acid using the reactive

crystallization method needs to be carried out more than once to meet the terephthalic acid requirements for PET polymerization.

CONCLUSION

The semi-batch reactive crystallization of terephthalic acid at constant pH and isothermal was conducted to study the effect of the crystallization processes (time, pH, temperature, concentration of secondary solutions, flow rate of secondary solutions, and stirring rate) on the CSD of terephthalic acid. The experimental results showed that the pH and concentration of reactants influenced CSD. The operational parameters of crystallization of time, temperature, flow rate, secondary solution, and stirring rate were found to have no significant effect on the mean crystal size of terephthalic acid. Crystallization of terephthalic acid was dominated by nucleation, which was reflected in the fine terephthalic acid crystal size. The semi-batch reactive crystallization with double-feeding reactants at constant pH and temperature forms nearly the same size crystals. However, purification by the reactive crystallization method needs to be carried out more than once to meet the TA requirements for PET polymerization.

ACKNOWLEDGMENTS

The authors thank *Kementerian Riset, Teknologi dan Pendidikan Tinggi via Saintek* Scholarship No. 3535 in 2018 for financial support. The authors also thank the Center for Standardization and Industrial Pollution Prevention Services and the Ministry of Industry for

providing research facilities.

■ AUTHOR CONTRIBUTIONS

Bekti Marlina was involved in conceptualization, methodology, formal analysis, data curation, writing of the draft, and visualization. Rochmadi contributed to conceptualization, methodology, resource acquisition, writing review, and editing and provided supervision. Hary Sulistyono participated in methodology, validation, writing review, and editing and provided supervision. All authors have carefully read and agreed to the final version of the manuscript.

■ REFERENCES

- [1] Cao, J., Meng, C., Cheng, X., and Pan, X., 2019, Surface alkali deweighting and dyeing of polyester fabric by one-bath and one-step process, *Surf. Innovations*, 7 (2), 104–111.
- [2] Gupta, D., Chaudhary, H., and Gupta, C., 2015, Topographical changes in polyester after chemical, physical and enzymatic hydrolysis, *J. Text. Inst.*, 106 (7), 690–698.
- [3] Hilal, N.M., Gomaa, S.H., and Elsisy, A.A., 2020, Improving dyeing parameters of polyester/cotton blended fabrics by caustic soda, chitosan, and their hybrid, *Egypt. J. Chem.*, 63 (6), 2381–2395.
- [4] Yang, B., Xu, H., Wang, J., Yan, D., Zhong, Q., and Yu, H., 2018, Performance evaluation of anaerobic baffled reactor (ABR) for treating alkali-decrement wastewater of polyester fabrics at incremental organic loading rates, *Water Sci. Technol.*, 77 (10), 2445–2453.
- [5] Chaonan, L., and Jihua, C., 2007, The study of the recovery of highly purified terephthalic acid from alkali weight-reduction wastewater, *Int. J. Environ. Pollut.*, 29 (4), 484–494.
- [6] Lewis, A.E., Seckler, M.M., Kramer, H., and Van Rosmalen, G., 2015, *Industrial Crystallization: Fundamentals and Applications*, Cambridge University Press, Cambridge, UK.
- [7] Lee, A.Y., Erdemir, D., and Myerson, A.S., 2019, "Crystals and Crystal Growth" in *Handbook of Industrial Crystallization*, Eds. Myerson, A.S., Erdemir, D., and Lee, A.Y., Cambridge University Press, Cambridge, UK, 32–75.
- [8] Nagy, Z.K., Fujiwara, M., and Braatz, R.D., 2019, "Monitoring and Advanced Control of Crystallization Processes" in *Handbook of Industrial Crystallization*, Eds. Myerson, A.S., Erdemir, D., and Lee, A.Y., Cambridge University Press, Cambridge, UK, 313–345.
- [9] Nicoud, L.H., and Myerson, A.S., 2019, "Influence of Impurities and Additives on Crystallization" in *Handbook of Industrial Crystallization*, Eds. Myerson, A.S., Erdemir, D., and Lee, A.Y., Cambridge University Press, Cambridge, UK, 115–135.
- [10] Suharso, S., Parkinson, G., and Ogden, M., 2007, effect of cetyltrimethylammonium bromide (CTAB) on the growth rate and morphology of borax crystals, *J. Appl. Sci.*, 7 (10), 1390–1396.
- [11] Karpiński, P.H., and Bałdyga, J., 2019, "Precipitation Processes" in *Handbook of Industrial Crystallization*, Eds. Myerson, A.S., Erdemir, D., and Lee, A.Y., Cambridge University Press, Cambridge, UK, 216–265.
- [12] Pitt, K., Peña, R., Tew, J.D., Pal, K., Smith, R., Nagy, Z.K., and Litster, J.D., 2018, Particle design via spherical agglomeration: A critical review of controlling parameters, rate processes and modelling, *Powder Technol.*, 326, 327–343.
- [13] Liu, F., Bagi, S.D., Su, Q., Chakrabarti, R., Barral, R., Gamekkanda, J.C., Hu, C., and Mascia, S., 2022, Targeting particle size specification in pharmaceutical crystallization: A review on recent process design and development strategies and particle size measurements, *Org. Process Res. Dev.*, 26 (12), 3190–3203.
- [14] Bałdyga, J., 2016, Mixing and fluid dynamics effects in particle precipitation processes, *KONA Powder Part. J.*, 33, 127–149.
- [15] Rewatkar, K., Shende, D.Z., and Wasewar, K.L., 2018, Reactive crystallization of calcium oxalate: Population balance modeling, *Chem. Biochem. Eng. Q.*, 32 (1), 11–18.

- [16] Caro, J.A., Woldehaimanot, M., and Rasmuson, Å.C., 2014, Semibatch reaction crystallization of salicylic acid, *Chem. Eng. Res. Des.*, 92 (3), 522–533.
- [17] Han, B., and Louhi-Kultanen, M., 2018, Real-time Raman monitoring of calcium phosphate precipitation in a semi-batch stirred crystallizer, *Cryst. Growth Des.*, 18 (3), 1622–1628.
- [18] Zhang, W., Zhang, F., Ma, L., Yang, J., Yang, J., and Xiang, H., 2019, Prediction of the crystal size distribution for reactive crystallization of barium carbonate undergrowth and nucleation mechanisms, *Cryst. Growth Des.*, 19 (7), 3616–3625.
- [19] Chen, P.C., Cheng, G.Y., Kou, M.H., Shia, P.Y., and Chung, P.O., 2001, Nucleation and morphology of barium carbonate crystals in a semi-batch crystallizer, *J. Cryst. Growth*, 226 (4), 458–472.
- [20] Tai, C.Y., and Chen, P.C., 1995, Crystal growth and agglomeration of calcium sulfite hemihydrate crystals, *Ind. Eng. Chem. Res.*, 34 (4), 1342–1351.
- [21] Slapnik, J., Kraft, G., Wilhelm, T., and Lobnik, A., 2019, Purification of Recycled Terephthalic Acid and Synthesis of Polyethylene Terephthalate, *The 1st International Conference on Circular Packaging*, Ljubljana, Slovenia, 151–159.
- [22] McDonald, M.A., Salami, H., Harris, P.R., Lagerman, C.E., Yang, X., Bommarius, A.S., Grover, M.A., and Rousseau, R.W., 2021, Reactive crystallization: A review, *React. Chem. Eng.*, 6 (3), 364–400.
- [23] Rezazadeh, A., Thomsen, K., Gavala, H.N., Skiadas, I.V., and Fosbøl, P.L., 2021, Solubility and freezing points of disodium terephthalate in water-ethylene glycol mixtures, *J. Chem. Eng. Data*, 66 (5), 2143–2152.
- [24] Christian, G.D., Dasgupta, P.K., and Schug, K.A., 2013, *Analytical Chemistry*, 7th Ed., John Wiley & Sons, Inc., Hoboken, New York, US.
- [25] Rehage, H., Semmel, M., and Kind, M., 2020, A dynamic model for process flowsheet simulation of semi-batch precipitation of sparingly soluble salts, *Comput. Chem. Eng.*, 137, 106818.
- [26] Amari, S., Sugawara, C., Kudo, S., and Takiyama, H., 2022, Investigation of operation strategy based on solution pH for improving the crystal quality formed during reactive crystallization of L-aspartic acid, *ACS Omega*, 7 (3), 2989–2995.
- [27] Sato, E., Seki, Y., and Takiyama, H., 2019, Control of reaction crystallization of organic compounds using the supersaturation profile, *J. Chem. Eng. Jpn.*, 52 (7), 599–604.
- [28] Utomo, J., Asakuma, Y., Maynard, N., Maeda, K., Fukui, K., and Tadé, M.O., 2010, Semi-batch reactive crystallisation of mono-ammonium phosphate: An experimental study, *Chem. Eng. J.*, 156 (3), 594–600.
- [29] Li, M., Shang, Z., and Hou, B., 2019, Optimizing the aspect ratio of cephalexin in reactive crystallization by controlling supersaturation and seeding policy, *Trans. Tianjin Univ.*, 25 (4), 348–356.
- [30] Park, C., and Sheehan, R.J., 2000, "Phthalic Acids and Other Benzenepolycarboxylic Acids" in *Kirk-Othmer Encyclopedia of Chemical Technology*, John Wiley & Son, New York.
- [31] Tourbin, M., Brouillet, F., Galey, B., Rouquet, N., Gras, P., Chebel, N.A., Grossin, D., and Frances, C., 2020, Agglomeration of stoichiometric hydroxyapatite: Impact on particle size distribution and purity in the precipitation and maturation steps, *Powder Technol.*, 360, 977–988.
- [32] Wiley-VCH, 2016, *Ullmann's Polymer and Plastics*, 1st Ed., Wiley-VCH, Weinheim, Germany.
- [33] Azarpour, A., Rezaei, N., and Zendejboudi, S., 2020, Product quality control in hydropurification process by monitoring reactor feed impurities: Dynamic mathematical modeling, *J. Ind. Eng. Chem.*, 92, 62–76.
- [34] Rao, P.N., Sabavath, G.K., and Paul, S.N., 2021, Impact of MTA blend % in melt spinning process and polyester properties, *SN Appl. Sci.*, 3 (2), 184.